isvr Institute of Sound and Vibration Research

Comparison of Two Wave Element Methods for the Helmholtz Problem

T. Huttunen, P. Gamallo and R.J. Astley

ISVR Technical Report No 307

November 2006

University of Southampton

SCIENTIFIC PUBLICATIONS BY THE ISVR

Technical Reports are published to promote timely dissemination of research results by ISVR personnel. This medium permits more detailed presentation than is usually acceptable for scientific journals. Responsibility for both the content and any opinions expressed rests entirely with the author(s).

Technical Memoranda are produced to enable the early or preliminary release of information by ISVR personnel where such release is deemed to the appropriate. Information contained in these memoranda may be incomplete, or form part of a continuing programme; this should be borne in mind when using or quoting from these documents.

Contract Reports are produced to record the results of scientific work carried out for sponsors, under contract. The ISVR treats these reports as confidential to sponsors and does not make them available for general circulation. Individual sponsors may, however, authorize subsequent release of the material.

Comparison of two wave element methods for the Helmholtz problem

T. Huttunen [a],

[a] *University of Kuopio, Department of Applied Physics, PO Box 1627, 70210 Kuopio, Finland*

P. Gamallo [b] and R. J. Astley [b]

[b] *Institute of Sound and Vibration Research, University of Southampton, Highfield Road, Southampton SO17 1BJ, UK*

Abstract

In comparison with low-order finite element methods, the use of oscillatory basis functions has been shown to reduce the computational complexity associated with the numerical approximation of Helmholtz problems at high wave numbers. We compare two different wave element methods for the 2D Helmholtz problems. The methods chosen for this study are the partition of unity finite element method (PUFEM) and the ultra-weak variational formulation (UWVF). In both methods, the local approximation of wave field is computed using a set of plane waves for constructing the basis functions. However, the methods are based on different variational formulations; and the PUFEM basis also includes a polynomial component whereas the UWVF basis consists purely of plane waves. As model problems we investigate propagating and evanescent wave modes in a duct with rigid walls; and singular eigenmodes in an L-shaped domain. Results show a good performance of both methods for the modes in the duct but only a satisfactory accuracy was obtained in the case of the singular field. On the other hand, the both methods can suffer from the ill-conditioning of the resulting matrix system.

Key words: Helmholtz problem, Partition of Unity, Ultra-weak variational formulation
PACS: 43.20.Mv, 02.70.Dh, 02.60.Cb

1 Introduction

A wide range of physical systems in steady-state oscillation can be characterized using the Helmholtz equation. Yet the numerical approximation of

Helmholtz problems poses a serious challenge to standard, low-order finite element techniques. Due to the requirement of dense spatial discretization, the modeling of wave fields at high wave numbers is computationally demanding when conventional polynomial finite elements are used. Approximability requirements are severe and these are exacerbated by cumulative phase and dispersion errors. This presents one of the unsolved problems of the finite element method [22].

A promising improvement for relaxing the mesh density of the finite element methods is the incorporation of the physical features of the solution into the approximation subspace. This approach has been utilized for the Helmholtz problem by locally approximating the solution as a superposition of propagating plane waves or by enriching the polynomial finite element basis function with the plane waves. The enriched methods include, for example, the partition of unity finite element method (PUFEM) [18,3], the generalized finite element method (GFEM) [21,2], which is a combination of the classical finite element method and the partition of unity method, and discontinuous enrichment method (DEM) [9]. A purely plane wave basis has been used, for example, with the ultra-weak variational formulation [6,7], discontinuous Galerkin method [10] and the least-squares method [19]. The aim of this study is to compare the PUFEM and UWVF for 2D Helmholtz problems. In particular, we shall extend PUFEM and UWVF simulations for problems including evanescent waves and singularities.

In the PUFEM, the polynomial finite element basis is multiplied by discrete plane waves. The method has been evaluated for the Helmholtz problem in [14,15] and the results show a notable reduction in the computational burden associated with the high frequency wave problem.

An improvement in computational efficiency compared to a low-order FEM is also observed with the DEM [9] in which the basis is constructed by adding plane wave solutions to the polynomial basis. The PUFEM and DEM, in addition to the generalized finite element method [21], are compared for a 1D flow acoustic problem in [2]. All methods give a tolerable accuracy when the number of degrees of freedom per wavelength is approximately 4 which is clearly below a common rule of thumb of 10 points per wavelength for the low-order FEM.

While having similarities with the PUFEM, the major differences of the ultra-weak variational formulation are a different underlying variational formulation and the construction of a basis using only plane waves. The UWVF was first introduced in general form in [8] and analyzed for the Helmholtz and time-harmonic Maxwell equations in [5–7]. The results obtained by the originators of the UWVF and in the subsequent study [13] show that the method permits the use of a relatively coarse mesh and, in comparison to conventional finite

elements, reduces the number of degrees of freedom per wavelength needed for tolerable accuracy.

Finally we note that although the simulations of this study focus on the Helmholtz equation, the wave basis methods which are presented are also used for a wider class of time-harmonic wave problems. The original work on the UWVF focused mainly on the solution of the 3D Maxwell equations [5]. Subsequently, the method has been also extended for elastic wave problems [12] and fluid-structure interaction problems [11]. On the other hand, the PUFEM has been applied to flow acoustics problems and proved to be far more efficient than standard finite element methods when applied to short wave acoustic propagation on uniform and nonuniform potential flows [2,1]. We therefore anticipate that the results obtained here will benefit other applications of wave elements methods.

2 Numerical methods for the Helmholtz model

2.1 Statement of the problem

The Helmholtz problem investigated in this study is now presented. Let Ω be a domain in $\mathbb{R}^2$ with the boundary Γ. Then a time-harmonic wave field with the wave number $\kappa \in \mathbb{R}$ satisfies the Helmholtz equation

$$\Delta u + \kappa^2 u = 0 \quad \text{in } \Omega, \tag{1}$$

$$(1+Q)\frac{\partial u}{\partial \nu} + (Q-1)i\kappa u = g \quad \text{on } \Gamma, \tag{2}$$

where the boundary condition (2), $Q \in \mathbb{C}$, gives either a Dirichlet when $Q = -1$, Neumann when $Q = 1$, or mixed, Robin-type boundary condition when $Q \neq 1, -1$ ($|Q| < 1$ for a strictly dissipative condition). The source term on the boundary is denoted by g.

Since the both methods investigated in this study use similar finite element meshes, a disjoint partition of the domain is defined so that $\Omega = \cup_{k=1}^{K} \Omega_k$. The number of vertices in the mesh is denoted by L.

2.2 Partition of unity finite element method

The Partition of Unity Method was proposed by Melenk and Babuška [18,3] as a general approach for enhancing the finite element solution of partial differen-

tial equations. PUFEM provides a framework for including information about the local behavior of the solution within the approximation subspace of a conventional FE discretisation, leading in theory to a better approximation of the underlying physics and to reduced CPU time and memory requirements. Recent studies [15,20,16] of homogeneous 2-D and 3-D Helmholtz problems have confirmed that very significant computational efficiencies can be achieved for short wave problems.

While providing an improved local approximation, the PUFEM retains in a global sense many of the attractive features of a conventional finite element model. It accommodates unstructured meshes and generates a trial solution which is continuous at all points in the solution domain. Most importantly, the nodal definition of the basis functions is preserved, which leads to sparse matrix systems. The flexibility which exists in the choice of local basis and shape functions also provides a natural way of tackling inhomogeneous problems by defining local approximations which vary over the solution domain.

In application to wave problems, local plane wave solutions are a natural choice for enriching the finite element trial space

$$\psi(x,y) = Ae^{-i\kappa(x\cos\theta + y\sin\theta)}, \quad \forall A \in \mathbb{C} \ \text{ and } \ \theta \in [0, 2\pi],$$

since they are solution of the homogeneous Helmholtz equation (1). The discrete trial space is built by selecting at each node ℓ of a conventional Finite Element mesh a *finite* number p_ℓ of wave directions which can vary from node to node. In all of the cases considered in this article the wave directions are chosen angularly equispaced. A uniform distribution is not mandatory. If there is *a priori* knowledge about the probable direction(s) of propagation at a particular node, this can be used to select a suitable set of wave functions for inclusion in the local approximation basis at that node.

A generic element ϕ_h of the PUFEM finite element space therefore takes the form

$$\phi_h(x,y) = \sum_{\ell=1}^{L} N_\ell(x,y) \sum_{n=1}^{p_\ell} A_{\ell,n}\, e^{-i\kappa(x\cos\theta_n + y\sin\theta_n)} \tag{3}$$

where L is the number of nodes in the mesh, and $\{A_{\ell,n}\}$ is a set of unknown nodal amplitudes which form the degrees of freedom of the model. The functions

$$N_\ell(x,y), \quad \ell = 1, 2, \ldots, L$$

are conventional finite element shape functions which satisfy the usual 'Partition of Unity' relationship that

$$\sum_{\ell=1}^{L} N_\ell(x,y) = 1.$$

Equation (3) can also be written as a double summation in terms of composite basis functions $\psi_{\ell,j}(x,y)$ which contain both the conventional shape functions and the discrete wave solutions, i.e.

$$\phi_h(x,y) = \sum_{\ell=1}^{L} \sum_{n=1}^{p_\ell} A_{\ell,n}\, \psi_{\ell,n}(x,y), \;\; \text{where } \psi_{\ell,n}(x,y) = N_\ell(x,y)\, e^{-i\kappa(x\cos\theta_n + y\sin\theta_n)}.$$

The PUFEM finite element space

$$\mathcal{V}_h := \{\phi_h \text{ eq.(3)} : A_{l,j} \in \mathbb{C}, \;\; \ell = 1,\ldots,L, \;\; j = 1,\ldots,p_\ell\}$$

is used to obtain an approximate solution to the problem posed by equations (1) and (2). In order to do that first we introduce the following sesquilinear and antilinear forms

$$\begin{aligned} a(u,\phi) &= \int_\Omega \nabla\bar{\phi}\cdot\nabla u - \kappa^2 \int_\Omega \bar{\phi}\, u - i\kappa \left(\frac{1-Q}{1+Q}\right) \int_{\Gamma_R} \bar{\phi}\, u \\ b(\phi) &= \frac{1}{2}\int_{\Gamma_N} \bar{\phi}\, g + \frac{1}{1+Q}\int_{\Gamma_R} \bar{\phi}\, g \end{aligned}$$

to write the weak formulation of problem (1)-(2)

$$a(u,\phi) = b(\phi), \;\; \forall \phi \in H^1_{\Gamma_D}(\Omega),$$

where Γ_N, Γ_R and Γ_D are Neumann, Robin-type, and homogeneous Dirichlet boundaries respectively, so that;

$$\begin{aligned} \frac{\partial u}{\partial \nu} &= \frac{g}{2} \quad \text{on } \Gamma_N, \\ \frac{\partial u}{\partial \nu} &= i\kappa \left(\frac{1-Q}{1+Q}\right) u + \frac{g}{1+Q} \quad \text{on } \Gamma_R, \\ u &= 0 \quad \text{on } \Gamma_D, \end{aligned}$$

where $\Gamma = \Gamma_N \cup \Gamma_R \cup \Gamma_D$, and

$$H^1_{\Gamma_D}(\Omega) := \left\{ v \in H^1(\Omega) : v\,|_{\Gamma_D} = 0 \right\}.$$

$H^1(\Omega)$ is the Sobolev space

$$H^1(\Omega) := \left\{ v \in L^2(\Omega) : \frac{\partial v}{\partial x_j} \in L^2(\Omega), \;\; j = 1,2 \right\}.$$

When an inhomogeneous Dirichlet condition is present, $u = g$ on Γ_D, it is easy to get a similar variational formulation by writing the solution as a sum of

functions $u = u_0 + u_D$, where u_D is any function in $H^1(\Omega)$ satisfying $u_D|_{\Gamma_D} = g$, and $u_0 \in H^1_{\Gamma_D}(\Omega)$ is the solution of the following variational problem

$$a(u_0, \phi) = b(\phi) - a(u_D, \phi), \ \forall \phi \in H^1_{\Gamma_D}(\Omega).$$

The PUFEM is based on a Galerkin type approximation of the above weak formulation. It is important to note that when Dirichlet conditions are present, the construction of the PUFEM approximation of $H^1_{\Gamma_D}(\Omega)$ is not as direct as for standard finite elements because, in general, the set of functions defined on Γ_D by the traces of the PUFEM basis functions are not linearly independent. The construction of the approximation of the space $H^1_{\Gamma_D}(\Omega)$ can be avoided by introducing Lagrange multipliers, to impose weakly the Dirichlet condition, and rewriting the weak formulation consistently. However, in the present work the space of admissible solutions $H^1_{\Gamma_D}(\Omega)$ is discretised with a PUFEM basis by considering the following subspace of PUFEM functions

$$\mathcal{V}_{h\Gamma_D} := \{\phi_h \in \mathcal{V}_h : \phi_h|_{\Gamma_D} = 0\}.$$

2.3 Ultra-weak variational formulation

We shall next briefly outline the ultra-weak variational formulation. The derivation of the UWVF in detail can be found from the reference [6]. Let us denote by $\Sigma_{k,j}$ the interface between elements Ω_k and Ω_j. For the UWVF, the original Helmholtz problem (1) is decomposed into sub-problems for each element Ω_k, $k = 1, \ldots, K$ so that

$$\Delta u_k + \kappa^2 u_k = 0 \qquad \text{in } \Omega_k \tag{4}$$

$$\frac{\partial u_k}{\partial \nu_k} - i\kappa u_k = -\frac{\partial u_j}{\partial \nu_j} - i\kappa u_j \qquad \text{on } \Sigma_{k,j} \tag{5}$$

$$\frac{\partial u_k}{\partial \nu_k} + i\kappa u_k = -\frac{\partial u_j}{\partial \nu_j} + i\kappa u_j \qquad \text{on } \Sigma_{k,j} \tag{6}$$

$$\left(\frac{\partial u_k}{\partial \nu_k} - i\kappa_k u_k\right) = Q\left(-\frac{\partial u_k}{\partial \nu_k} - i\kappa_k u_k\right) + g \qquad \text{on } \Gamma_k \tag{7}$$

The function to be solved in the UWVF is defined on the element boundaries as

$$\chi_k = \left(-\frac{\partial u_k}{\partial \nu_k} - i\kappa u_k\right)\Big|_{\partial\Omega_k}, \quad 1 \le k \le K. \tag{8}$$

In [6] the decomposed problem (4)-(7) and integration by parts are used to show that χ_k satisfies

$$\sum_{k=1}^{K}\int_{\partial\Omega_k}\frac{1}{\kappa}\chi_k\overline{\left(-\frac{\partial v_k}{\partial\nu_k}-i\kappa v_k\right)}-\sum_{k=1}^{K}\sum_{j=1}^{K}\int_{\Sigma_{k,j}}\frac{1}{\kappa}\chi_j\overline{\left(\frac{\partial v_k}{\partial\nu_k}-i\kappa v_k\right)}$$
$$-\sum_{k=1}^{K}\int_{\Gamma_k}\frac{Q}{\kappa}\chi_k\overline{\left(\frac{\partial v_k}{\partial\nu_k}-i\kappa v_k\right)}=\sum_{k=1}^{K}\int_{\Gamma_k}\frac{1}{\kappa}g\overline{\left(\frac{\partial v_k}{\partial\nu_k}-i\kappa v_k\right)}, \tag{9}$$

where v_k satisfies the local adjoint Helmholtz equation

$$\Delta v_k+\overline{\kappa}^2 v_k=0 \quad \text{in } \Omega_k. \tag{10}$$

Here the overbars refer to complex conjugation. The equation (9) is called the ultra-weak variational formulation of the Helmholtz equation.

The discrete UWVF results in by approximating the function χ_k using a superposition of propagating plane waves

$$\chi_k^a=\sum_{n=1}^{p_k}\chi_{k,n}\left(-\frac{\partial\psi_{k,n}}{\partial\nu_k}-i\kappa\psi_{k,n}\right), \tag{11}$$

where the plane wave basis functions can be written as

$$\psi_{k,n}=\begin{cases}e^{i\kappa(x\cos\theta_n+y\sin\theta_n)} & \text{in } \Omega_k\\ 0 & \text{elsewhere.}\end{cases}$$

As for the PUFEM, the propagation directions θ_n of the waves are chosen angularly equispaced on the unit circle. The numbers of basis directions p_k can vary between elements Ω_k, $k=1,...,K$.

By substituting the discrete approximation of χ_k (11) into the UWVF equation (9) and by setting $v_k=\psi_{k,n}$, the discrete UWVF can solved in the matrix form as

$$(D-C)X=b, \tag{12}$$

from which the weights $X=(\chi_{1,1},\chi_{1,2},..)^T$ for the basis functions can be solved.

The structure of elements in the matrices D and C; and the right hand side b are given in detail in [6] and [13]. The discrete UWVF equation (12) can be also written in an alternative, preconditioned form

$$(I-D^{-1}C)X=D^{-1}b, \tag{13}$$

which is generally preferred due to the improved conditioning of the problem [6],[13]. The latter form is particularly useful when large-scale problems are solved using iterative methods. In this study, the both forms (12) and (13) are used to resolve the UWVF approximations.

3 Numerical simulations

The coding of both methods is done in Matlab and the resulting systems of linear equations are solved using Matlab's backslash, i.e. by Gaussian elimination. A lower bound for the 1-norm condition number of the matrices is computed by means of the function *condest* of Matlab.

3.1 Wave propagation in a duct with rigid walls

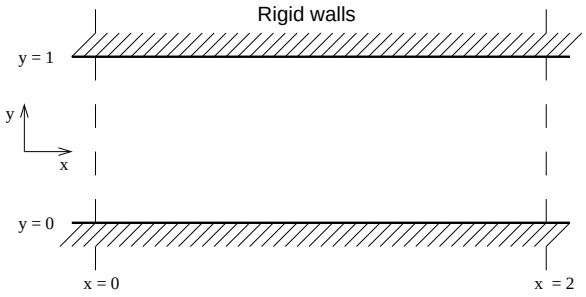

Fig. 1. Duct domain.

The first model problem consists of a rigid wall duct $\Omega \in [0,2] \times [0,1]$ with the outward boundary unit normal ν (see Figure 1). We analyze the following Helmholtz problem for the acoustic pressure u and associated boundary conditions

$$\begin{aligned}
\Delta u + \kappa^2 u &= 0 \quad \text{in } \Omega, \\
\frac{\partial u}{\partial \nu} &= \cos(m\pi y) \quad \text{on } x = 0,\ m \in \mathbb{N} \\
\frac{\partial u}{\partial \nu} + i\kappa u &= 0 \quad \text{on } x = 2 \\
\frac{\partial u}{\partial \nu} &= 0 \quad \text{on } y = 0, 1.
\end{aligned}$$

The inlet boundary $x = 0$ has an inhomogeneous Neumann condition and the outlet boundary $x = 2$ is characterized using an absorbing boundary condition. The boundaries $y = 0, 1$ are assumed perfectly rigid leading to vanishing normal derivatives on the boundary.

The exact solution for the problem can be obtained in the closed form as

$$u_{\text{ex}}(x, y) = \cos(m\pi y)(A_1 e^{-i\kappa_x x} + A_2 e^{i\kappa_x x})$$

where $\kappa_x = \sqrt{\kappa^2 - (m\pi)^2}$ and coefficients A_1 and A_2 satisfy the equation

$$i \begin{pmatrix} \kappa_x & -\kappa_x \\ (\kappa - \kappa_x)e^{-2i\kappa_x} & (\kappa + \kappa_x)e^{2i\kappa_x} \end{pmatrix} \begin{pmatrix} A_1 \\ A_2 \end{pmatrix} = \begin{pmatrix} 1 \\ 0 \end{pmatrix}$$

The solution represents propagating modes when the mode number m is below the cut-off value

$$m \leq m_{\text{cut-off}} = \frac{\kappa}{\pi}.$$

The modes for which $m > m_{\text{cut-off}}$ are evanescent. We compute numerical approximations for the highest propagating mode and the two lowest evanescent modes. To measure the accuracy of the numerical solution u_h, we introduce the following L_2 error,

$$\text{Error}(\%) := 100 \, \frac{\|u_{\text{ex}} - u_h\|_{L_2(\Omega)}}{\|u_{\text{ex}}\|_{L_2(\Omega)}}$$

The simulations are performed for the wave numbers $\kappa = 20, 40$ and 80 when the corresponding highest propagating mode numbers are $m = 6, 12$ and 25.

The meshes used in the simulation are shown in Fig. 2. The maximum element size $h_{\max}$ for the meshes is computed as the length of the longest edge of an element in the mesh.

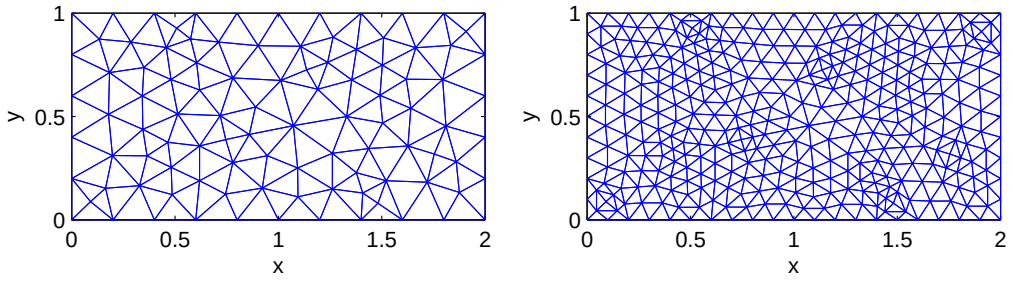

Fig. 2. The meshes used in the simulations. The mesh of the left has 100 vertices, 168 elements and $h_{\max}$=0.26. The finer mesh on the right consists of 367 vertices, 672 elements and has $h_{\max}$=0.13. The maximum element size $h_{\max}$ refers to the length of the longest edge of an element in the mesh.

Tables 1 and 2 summarize the PUFEM and UWVF results for the wave number $\kappa = 20$. We list the approximation error for the mode numbers $m = 6, 7$ and 8, the number of degrees of freedom (DOF), condition number (Cond) and the number of nonzero elements in the resulting matrix system (Nnz) as the function of basis dimension $p = p_k = p_\ell$ and maximum element size $h_{\max}$. In these simulations the basis dimension p is same in all elements.

In Table 2 the subscripts 1 and 2 in the condition number (Cond) and the number of nonzeros of the matrix system (Nnz) refer to the two forms of the UWVF matrix equation (12) and (13), respectively.

The results of Tables 1 and 2 suggest that the PUFEM provides a better accuracy than the UWVF whereas the UWVF is better conditioned than the PUFEM. In addition, there is a notable improvement in the conditioning of the UWVF equation when the preconditioned form (13) is used (Cond_2 in the table). The number of degrees of freedom associated for a fixed mesh and basis dimension is lower for the PUFEM. But the reason for this is evident. The degrees of freedom in the PUFEM are associated with element vertices so that total DOF is $\sum_{\ell=1}^{L} p_\ell$, where p is the dimension of the basis and L is the number of vertices in the mesh. However, the degrees of freedom in the UWVF are defined for element edges and therefore the DOF is $\sum_{k=1}^{K} p_k$, where K is the number of elements.

Nevertheless, the overall memory storage needed for the solution of the problem is not only dependent on DOFs but also on the number of nonzero elements in the corresponding matrix system (Nnz). The comparison of Nnz reveals that PUFEM and unpreconditioned UWVF have a comparable number of nonzeros but the preconditioned UWVF matrix equation has the lowest value of Nnz.

The results for the wave number $\kappa = 40$ are listed in Tables 3 and 4; and for the wave number $\kappa = 80$ in Tables 5 and 6. At $\kappa = 40$, the accuracy of the UWVF becomes comparable to that of the PUFEM. A further increase in κ (Tables 5 and 6) makes UWVF the most accurate of the two methods.

It is interesting that despite the UWVF matrix system (13) having a condition number two orders lower than the unpreconditioned form (13), the accuracy of the solution of (13) deteriorates earlier than for (12). The reason for this is, however, most likely in the two step inversion of the UWVF equation used in (13). It is shown earlier (see e.g. [13]) that the condition of subblocks D_k, and therefore the conditioning of D, closely follows the conditioning of the overall matrix system $I - D^{-1}C$. Then, the inversion of D at high condition numbers is inaccurate which deteriorates the solution of corresponding matrix equation (13) leading to poorer accuracy.

The tables for UWVF results list the accuracy with the unpreconditioned equation. Since the accuracy obtained from the two forms of the UWVF equa-

Table 1
PUFEM results for $\kappa = 20$.

		Error (%)					
p	$h_{\max}$	$m = 6$	$m = 7$	$m = 8$	DOF	Cond	Nnz
8	0.26	3.74	0.80	3.17	800	6.9e4	0.4e5
12	0.26	1.19e-2	9.37e-2	0.40	1200	8.3e7	0.9e5
4	0.13	7.90	1.77	3.53	1468	5.9e3	0.4e5
8	0.13	3.87e-2	4.14e-2	0.16	2936	3.7e7	1.6e5

Table 2
UWVF results for $\kappa = 20$.

		Error (%)							
p	$h_{\max}$	$m = 6$	$m = 7$	$m = 8$	DOF	Cond_1	Cond_2	Nnz_1	Nnz_2
8	0.26	23.9	9.15	30.4	1344	5.9e4	5.6e3	0.4e5	0.3e5
12	0.26	5.07e-2	0.41	2.17	2016	4.5e8	4.8e5	0.9e5	0.7e5
4	0.13	101.5	33.6	44.4	2688	1.3e3	1.7e3	0.4e5	0.3e5
8	0.13	0.66	0.74	1.93	5376	1.3e7	8.6e4	1.7e5	1.3e5

tion differ at high condition numbers, when the error is different, the errors for preconditioned form is given below the tables 4 and 6.

It is clear that the accuracy of the PUFEM and UWVF approximations are comparable for a given problem size and can be improved either by increasing the number of basis functions (a p-refinement) or by refining the mesh (a h-refinement). In Fig. 3, we compare these two approaches for the duct problem at the wave number $\kappa = 40$. The UWVF results are computed by solving the discrete equation in the form (13). Results for both the propagating ($m = 12$) and the evanescent mode ($m = 13$) show that the most memory efficient increase in accuracy is obtained via the p-refinement. Yet this approach also leads to a more severe deterioration of the conditioning of the problem.

4 A singular problem

The second model problem is a singular eigenmode of the Helmholtz problem in an L-shaped domain, see Fig 4. The exterior boundary Γ is divided into two parts $\Gamma = \Gamma_1 \cup \Gamma_2$ so that the edges meeting at the origin are denoted by Γ_1 and the rest of the boundary Γ constitutes Γ_2.

We seek the solution of the problem

Table 3
PUFEM results for $\kappa = 40$.

		Error (%)					
p	$h_{\max}$	m=12	m=13	m=14	DOF	Cond	Nnz
12	0.26	26.7	56.0	170	1200	1.3e6	0.9e5
16	0.26	6.19e-2	1.32	4.10	1600	4.0e6	1.6e5
20	0.26	9.43e-4	3.43e-2	0.60	2000	1.6e9	2.5e5
8	0.13	38.5	0.29	4.02	2936	5.0e4	1.6e5
12	0.13	2.85e-2	2.08e-2	0.12	4404	4.6e7	3.5e5

Table 4
UWVF results for $\kappa = 40$.

		Error (%)							
p	$h_{\max}$	m=12	m=13	m=14	DOF	Cond_1	Cond_2	Nnz_1	Nnz_2
12	0.26	33.1	9.58	73.7	2016	2.5e5	1.8e4	0.9e5	0.7e5
16	0.26	5.50e-2	0.28	1.52	2688	7.0e8	7.4e5	1.6e5	1.3e5
20	0.26	7.93e-4[a]	1.18e-2	0.11	3360	6.8e12	1.1e9	2.6e5	2.0e5
8	0.13	53.1	6.16	21.3	5376	9.0e4	2.3e4	1.7e5	1.3e5
12	0.13	9.65e-2	0.12	0.54	8064	7.1e8	2.5e6	3.8e5	3.0e5

1.66e-3[a] (the corresponding error when the UWVF is solved using the preconditioned equation (13))

$$\begin{aligned} \Delta u + \kappa^2 u &= 0 \quad \text{in } \Omega, \\ u &= 0 \quad \text{on } \Gamma_1, \\ \frac{\partial u}{\partial \nu} + i\kappa u &= \frac{\partial g}{\partial n} + i\kappa g \quad \text{on } \Gamma_2, \end{aligned}$$

where

$$g(r,\theta) = J_{2/3}(\kappa r)\sin\left(\frac{2}{3}\theta\right).$$

The exact solution of the problem is $u_{\text{ex}} = g$. This solution has a singular derivative at the origin.

Two meshes are used in the simulation. The first, labeled with M_1, has nearly equal sized elements and the second mesh M_2 is refined near the origin. Figures 5 and 6 show the error of PUFEM and UWVF as the function of conditioning and the number of nonzeros of the matrix equation for $\kappa = 40$. The results for both meshes are presented in the same figures. In addition, two forms of the matrix equation (Equations (12) and (13)) are used in the case of the UWVF.

Table 5
PUFEM results for $\kappa = 80$.

		Error (%)					
p	$h_{\max}$	m=25	m=26	m=27	DOF	Cond	Nnz
24	0.26	37.2	33.1	57.2	2400	2.1e4	3.7e5
28	0.26	1.22	8.86	19.1	2800	2.7e8	5.0e5
32	0.26	1.42e-3	3.76	5.71	3200	2.3e10	6.5e5
16	0.13	9.28	3.64	4.46	5872	8.8e6	6.3e5
20	0.13	7.42e-2	0.59	0.81	7340	1.5e9	9.8e5

Table 6
UWVF results for $\kappa = 80$.

		Error (%)							
p	$h_{\max}$	m=25	m=26	m=27	DOF	Cond_1	Cond_2	Nnz_1	Nnz_2
24	0.26	0.59	1.12	4.54	4032	2.4e10	1.3e7	3.7e5	2.9e5
28	0.26	8.30e-3[b]	7.82e-2	0.34	4704	7.0e13	1.2e10	5.0e5	4.0e5
32	0.26	7.80e-5[c]	6.98e-3[d]	3.71e-2[e]	5376	1.3e17	8.8e12	6.6e5	5.2e5
16	0.13	0.47	0.36	0.95	10752	1.2e9	3.9e6	6.7e5	5.2e5
20	0.13	3.43e-3[f]	1.63e-2	6.00e-2	13440	9.9e12	1.1e10	1.1e6	8.1e5

1.68e-2[b], 29.5[c], 1.11[d], 4.56[e], 4.12e-3[f] (the corresponding errors when the UWVF is solved using the preconditioned equation (13))

Results suggest that both methods suffer from ill-conditioning before high accuracy levels (say $< 1\%$) are reached. The smallest errors are obtained by using the refined mesh M_2 (in the case of UWVF only unpreconditioned equation gives improved accuracy). For the coarser mesh M_1, the accuracy almost levels off until conditioning starts to increase the error.

In Fig. 7 we show the error and conditioning of the PUFEM and UWVF approximations as a function of the wave number. The results are computed in the coarse mesh M_1 and by using the basis dimension $p_k = p_\ell = 24$. The UWVF is again more sensitive for ill-conditioning which deteriorates the accuracy at the lowest wave number. On the other hand, it is interesting to observe the similarity of the conditioning of PUFEM and unpreconditioned UWVF.

Since the ill-conditioning appears to be the major factor for deteriorating the error and it evidently stems from the use of large number of basis functions in small element, we analyze next two strategies for choosing the basis. In Fig. 8, the error is plotted as a function of the conditioning and the number of nonzeros when the number basis functions is same in all elements or when the basis dimension varies from element to element (or from node to node).

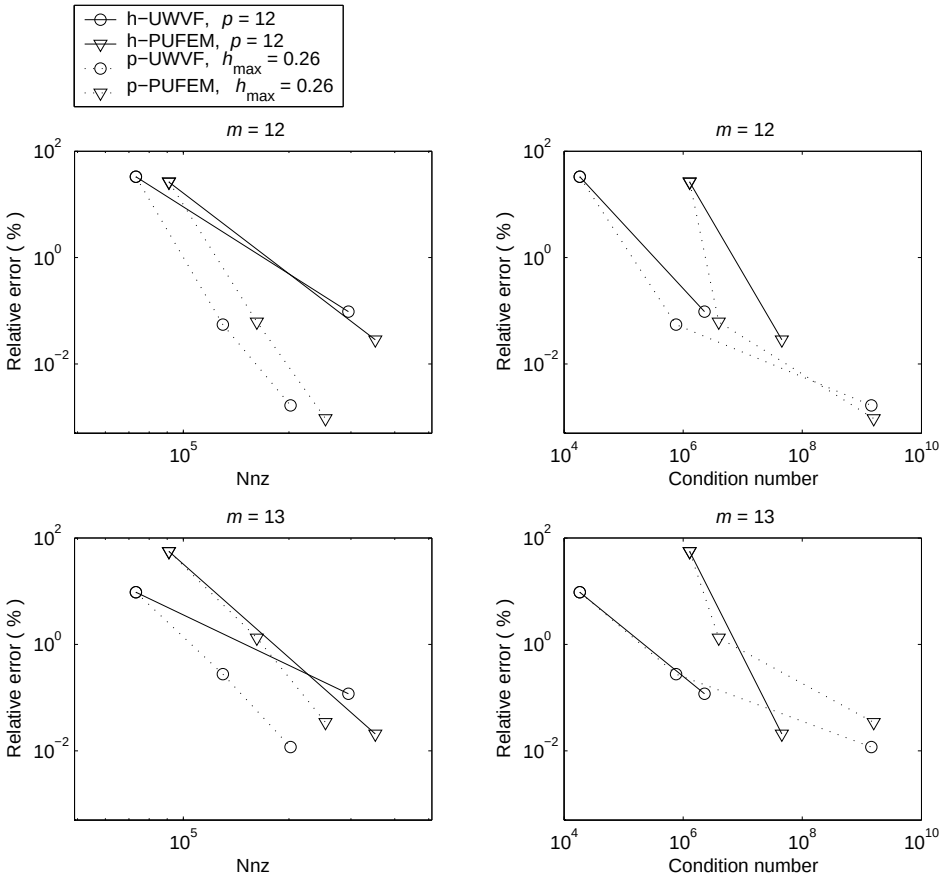

Fig. 3. A comparison of the two strategies for improving the accuracy. The errors presented using solid lines are computed by refining the mesh and using a fixed number of basis functions ($p_k = 12$) (we call this approach by h-UWVF and h-PUFEM). Dotted line errors are computed in the coarser mesh ($h_{\max} = 0.26$) and by increasing the basis dimension (p-UWVF and p-PUFEM). The results are shown for the wave number $\kappa = 40$ and for the modes $m = 12$ (first row) and $m = 13$ (second row).

For the UWVF, the element size h_k for an element Ω_k is the length of the longest edge of the element. And the number of basis functions p_k for the element Ω_k is computed as

$$p_k = \text{round}\left[\kappa h_k + C(\kappa h_k)^{1/3}\right], \tag{14}$$

where the constant C is chosen as $C = 3, 4, ..., 14$ (however, in Fig. 8 the accuracy of the UWVF started to deteriorate before the largest C values). This formula for the basis dimension stems from the analysis of truncation of the Jacobi-Anger series in the context of the fast multipole method [4]. It can be expected that a similar analysis is needed for studying the approximating properties of plane waves. In this point and in this context, however, the formula (14) is used without a rigorous mathematical analysis of its validity.

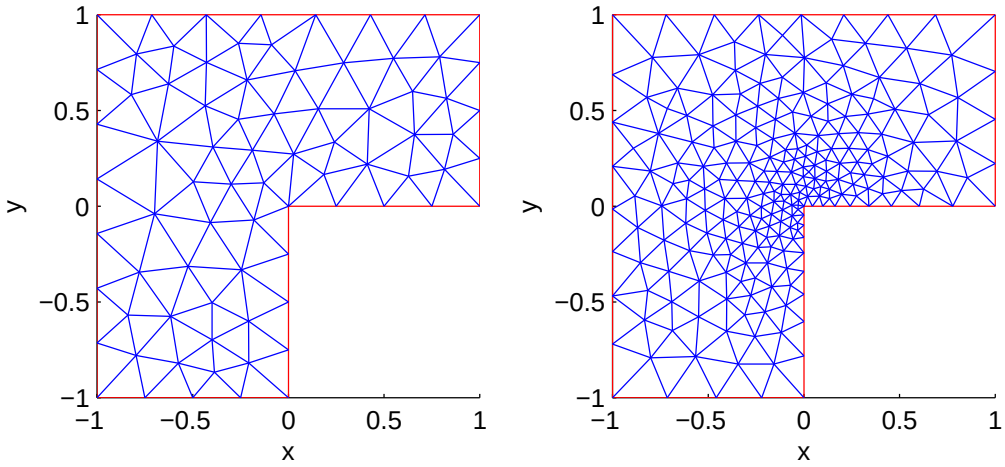

Fig. 4. The meshes for the L-shaped domain. *Left:* Mesh M_1 consisting of 78 vertices, 124 elements and having $h_{\max} = 0.38$. *Right:* Mesh M_2 consisting of 233 vertices, 422 elements and having $h_{\max} = 0.31$.

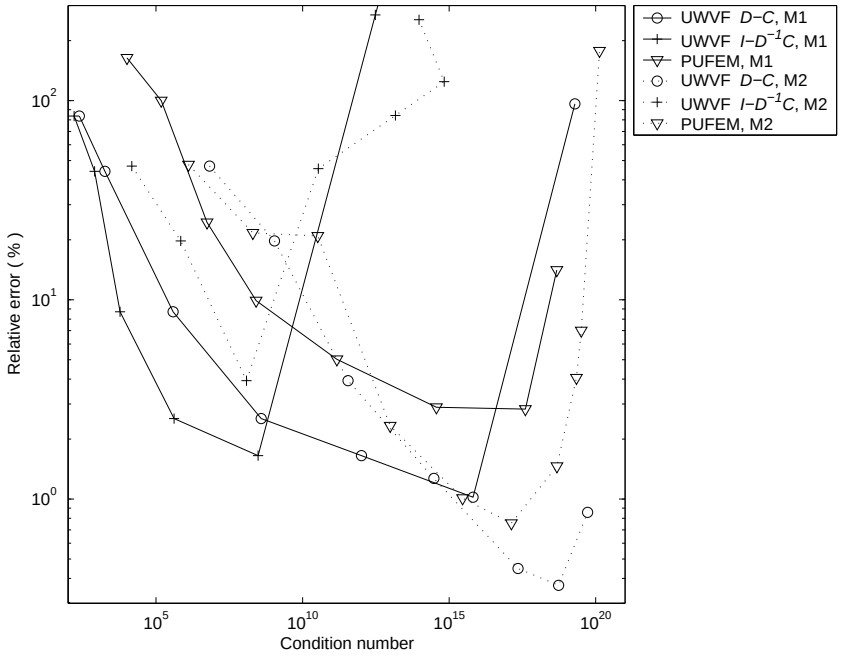

Fig. 5. The error of the PUFEM and UWVF approximation as a function of the condition number of the corresponding matrix equations. Two forms (12) and (13) are used for solving the UWVF problem. In addition, results are shown for two different meshes, see Fig. 4.

For the PUFEM, the number of directions is chosen by using a similar formula

$$p_\ell = \text{round}\left[\kappa h_\ell + C(\kappa h_\ell)^{1/3}\right]. \tag{15}$$

In the PUFEM, however, the degrees of freedom are associated with the el-

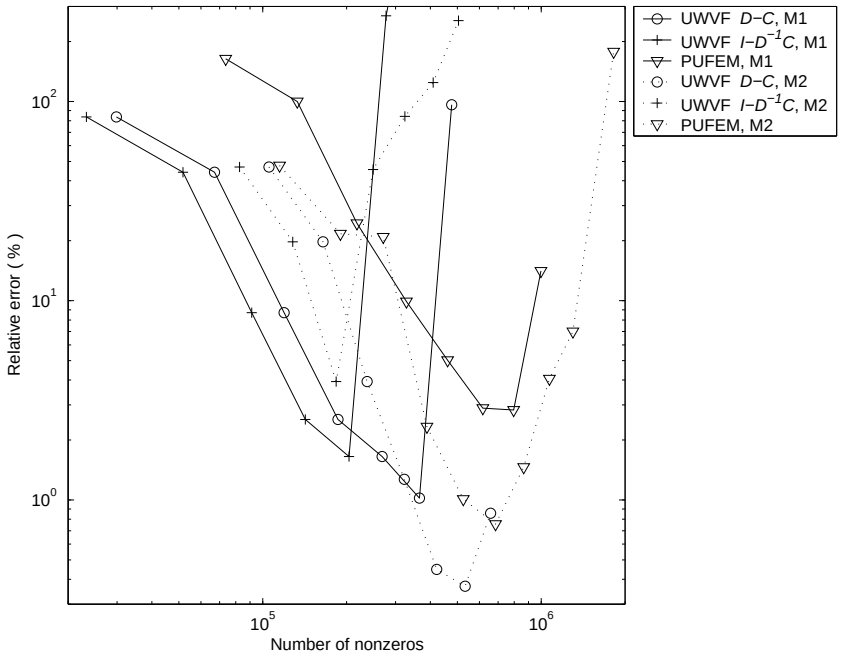

Fig. 6. The error of the PUFEM and UWVF approximation as a function of nonzeros elements in the corresponding matrix equations.

ement vertices. Then, p_ℓ denotes the number of directions at the ℓ'th node. Correspondingly, h_ℓ is the longest element edge coming out of the ℓ'th node. The parameter C is the same as for the UWVF.

The graphs of Fig. 8 show that the use of nonuniform number of basis functions notably improves the conditioning of both methods. In particular, the accuracy with the nonuniform basis is much better if we compare the errors in the region where the condition numbers are below 10^{12}. When one allows condition numbers that are higher than 10^{12}, the benefit of the nonuniform basis starts to vanish. In fact, the most accurate approximation is obtained by using unpreconditioned UWVF with an equal number of basis directions in each element. But it is also interesting to observe that with the nonuniform basis, the accuracy of PUFEM and unpreconditioned UWVF approximations is slightly less sensitive to ill-conditioning, that is, the error as a function of the condition number using the nonuniform basis decreases little longer than with the uniform basis.

In the case of PUFEM and unpreconditioned UWVF, the improved conditioning comes with the price of the increased matrix storage needed to obtain highest level of accuracy. The benefit of the nonuniform basis is the most evident with the preconditioned UWVF since it suffers earlier from the ill-conditioning caused by the uniform basis.

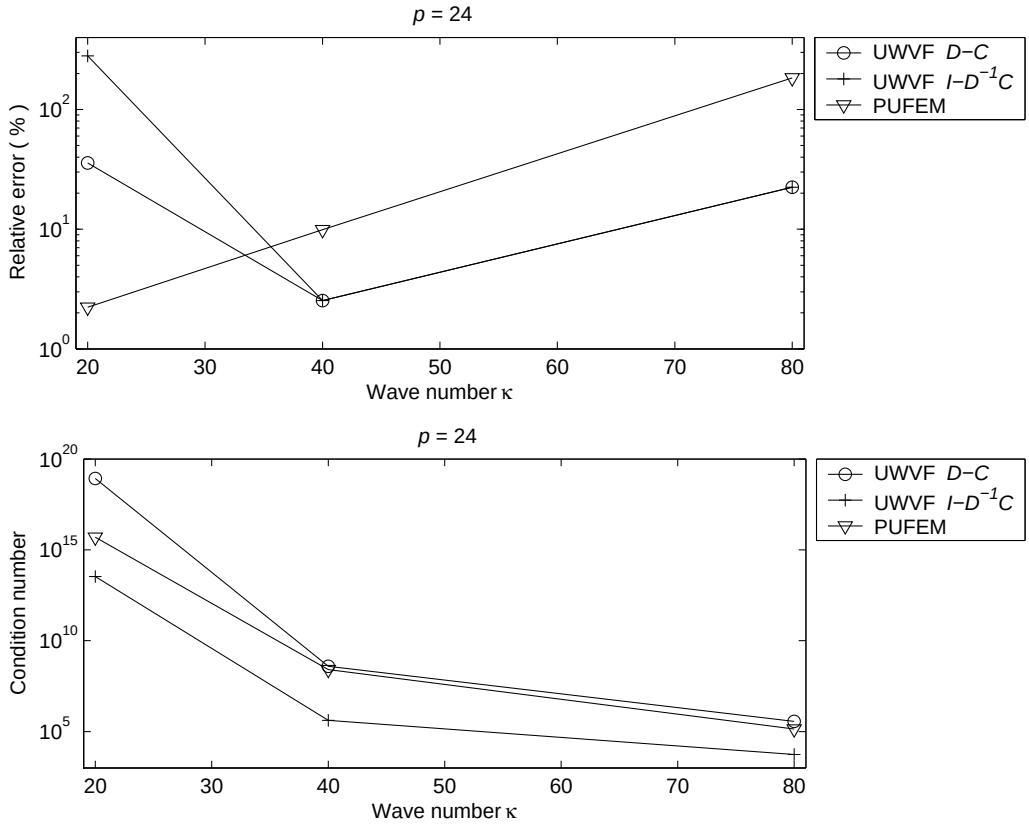

Fig. 7. The error as a function of the wave number κ for a fixed number of basis functions $p = 24$ and in the mesh M_1.

5 Discussion and conclusions

We compared two wave element methods for solving Helmholtz problems in 2D. The methods chosen for this study were the partition of unity finite element method (PUFEM) and the ultra-weak variational formulation (UWVF). We investigated the performance of the methods for simulating propagating and evanescent modes in a rigid wall duct; and singular eigenmodes in an L-shaped domain.

Both PUFEM and UWVF resulted in a high level accuracy for the propagating modes even if the meshes used in computations were relatively coarse (e.g. it was possible to obtain errors below 0.01% in meshes for which $\lambda/h \approx 0.3$). The error increased in the case of evanescent modes but, in most cases, remained on a tolerable level. A general trend was the UWVF performed better at higher frequencies whereas the PUFEM was more accurate at the low frequency. On the other hand, the PUFEM has a lower condition number at the highest frequency, even compared with the preconditioned form of the UWVF. It was observed that care must be taken of the form in which the discrete UWVF is solved. While the preconditioned form (13) has a lower condition number its

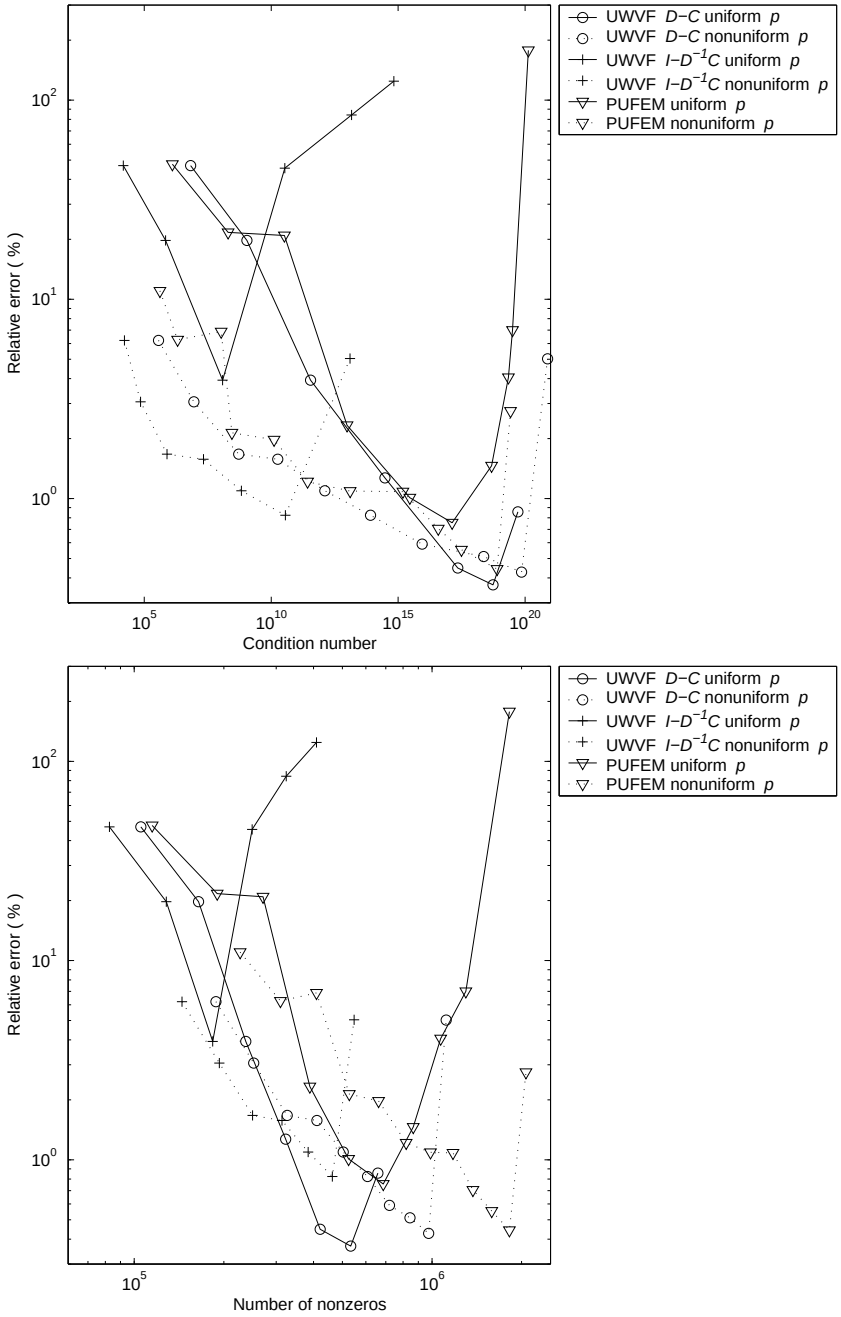

Fig. 8. Comparison of two approaches for choosing the number of plane wave basis functions. In the case of *uniform p*, the basis dimension is same throughout the whole computational domain Ω. The curves labeled with *nonuniform p* are computed so that the basis dimension p varies within the computational domain. The number of basis functions for the UWVF and PUFEM are computed from the formulas (14) and (15), respectively. Results are computed in the mesh M_2.

accuracy starts to deteriorate before that of the unpreconditioned equation (12).

The performance of the both methods for the singular problem was only sat-

isfactory. In the coarse mesh, it was impossible to obtain an error below 1% whereas the refinement of the mesh near the singularity improved the accuracy (the smallest errors in the refined mesh were about 0.4 %). The refinement of the mesh also led to a severe ill-conditioning of the problem if an equal number of basis functions was used in all elements. The conditioning was improved by letting the basis dimension to vary from node to node (or from element to element in the UWVF). The basis dimension was chosen by using an *ad hoc* formula which took into account the scaled wave number in each element.

We wish to remind that the formula we used for choosing the varying number of basis functions has not been proven to be optimal for this purpose. But the results suggest that by allowing the basis dimension to vary, it is possible to control the conditioning of the resulting matrix equations. The need of a low condition number becomes more important when iterative methods are used for solving the matrix systems. In the case of ill-conditioned problems, iterations may not converge.

To further increase the accuracy in the singular problem, one should use even more refined meshes or possibly use alternative basis functions which better imitate the solution near the singularity. For example, the use of Bessel function type basis near the singularity might, at least in part, compensate the need of mesh refinement. This possibility, however, was not investigated in this study.

This study was also limited in problems with constant material parameters. Yet, the both methods can be extended for problems with jumps in material parameters (see e.g. [17] and [13]). In the PUFEM, this is done using the Lagrange multipliers whereas in UWVF the extension is needs only minor modifications to the form used in this study.

6 Acknowledgments

Authors wish to thank Professor Peter Monk for suggesting the analysis of the evanescent modes and the singular problem. The work of Tomi Huttunen is funded by Nokia Research Center, Helsinki, Finland.

References

[1] R.J. Astley and P. Gamallo. The partition of unity finite element method for short wave acousitc propagation on nonuniform flows. *AIAA 2004-2893 of the 10th AIAA/CEAS Aeroacoustics Conference in Manchester, UK, May 2004.*

[2] R.J. Astley and P. Gamallo. Special short wave elements for flow acoustics. *Computer Methods in Applied Mechanics and Engineering*, 194:341–353, 2005.

[3] I. Babuška and J.M. Melenk. The partition of unity method. *International Journal for Numerical Methods in Engineering*, 40:727–758, 1997.

[4] Q. Carayol and F. Collino. Estimates in the fast multipole method for scattering problems Part 1: Truncation of the Jacobi-Anger series. *ESAIM: Mathematical Modeling and Numerical analysis*, 38(2):371–394, 2004.

[5] O. Cessenat. *Application d'une nouvelle formulation variationelle des equations d'ondes harmonigues, Problemes de Helmholtz 2D et de Maxwell 3D.* PhD thesis, Paris IX Dauphine, 1996.

[6] O. Cessenat and B. Després. Application of an ultra weak variational formulation of elliptic PDEs to the two-dimensional Helmholtz problem. *SIAM Journal of Numerical Analysis*, 35(1):255–299, 1998.

[7] O. Cessenat and B. Després. Using plane waves as base functions for solving time harmonic equations with the ultra weak variational formulation. *Journal of Computational Acoustics*, 11(2):227–238, 2003.

[8] B. Després. Sur une formulation variationnelle de type ultra-faible. *Comptes Rendus de l'Academie des Sciences - Series I*, 318:939–944, 1994.

[9] C. Farhat, I. Harari, and L. Franca. The discontinuous enrichment method. *Computer Methods in Applied Mechanics and Engineering*, 190:6455–6479, 2001.

[10] C. Farhat, I. Harari, and U. Hetmaniuk. A discontinuous Galerkin method with Lagrange multipliers for the solution of Helmholtz problems in the mid-frequency regime. *Computer Methods in Applied Mechanics and Engineering*, 192:1389–1419, 2003.

[11] T. Huttunen, J.P. Kaipio, and P. Monk. An ultra-weak method for fluid-structure interaction. Manuscript, 2005.

[12] T. Huttunen, P. Monk, F. Collino, and J.P. Kaipio. The ultra weak variational formulation for elastic wave problems. *SIAM Journal on Scientific Computing*, 25(5):1717–1742, 2004.

[13] T. Huttunen, P. Monk, and J.P. Kaipio. Computational aspects of the ultra-weak variational formulation. *Journal of Computational Physics*, 182:27–46, 2002.

[14] O. Laghrouche and P. Bettess. Short wave modelling using special finite elements. *Journal of Computational Acoustics*, 8(1):189–210, 2000.

[15] O. Laghrouche, P. Bettess, and R.J. Astley. Modelling of short wave diffraction problems using approximating systems of plane waves. *International Journal for Numerical Methods in Engineering*, 54:1501–1533, 2002.

[16] O. Laghrouche, P. Bettess, E. Perrey-Debain, and J. Trevelyan. Plane wave basis for wave scattering in three dimensions. *Commun. Numer. Meth Engng.*, 19:715–723, 2003.

[17] O. Laghrouche, P. Bettess, E. Perrey-Debain, and J. Trevelyan. Wave interpolation finite elements for helmholtz problems with jumps in the wave speed. *Computer Methods in Applied Mechanics and Engineering*, 194:367–381, 2005.

[18] J.M. Melenk and I. Babuška. The partition of unity finite element method: Basic theory and applications. *Comput. Methods Appl. Mech. Engrg.*, 139:289–314, 1996.

[19] P. Monk and D. Wang. A least squares method for the Helmholtz equation. *Computer Methods in Applied Mechanics and Engineering*, 175:121–136, 1999.

[20] P. Ortiz and E. Sanchez. An improved partition of unity finite element model for diffraction problems. *Int. Jour. Num. Meth. Eng.*, 50:2727–2740, 2001.

[21] T. Strouboulis, I. Babuška, and K. Copps. The design and analysis of the generalized finite element method. *Computer Methods in Applied Mechanics and Engineering*, 181:43–69, 2000.

[22] O. C. Zienkiewicz. Achievements and some unsolved problems of the finite element method. *International Journal for Numerical Methods in Engineering*, 47:9–28, 2000.